DOI: 10.1002/chem.200600777

Redox-Controlled Interaction of Biferrocenyl-Terminated Dendrimers with β-Cyclodextrin Molecular Printboards

Christian A. Nijhuis,[a] Karolina A. Dolatowska,[a] Bart Jan Ravoo,*[a] Jurriaan Huskens,[b] and David N. Reinhoudt*[a]

Abstract: This paper describes the synthesis and electrochemistry of biferrocenyl-terminated dendrimers and their β-cyclodextrin (β-CD) inclusion complexes in aqueous solution and at surfaces. Three generations of poly(propylene imine) (PPI) dendrimers, decorated with 4, 8, and 16 biferrocenyl (BFc) units, respectively, were synthesized. A water-soluble BFc derivative forms stable inclusion complexes with β-CD. The intrinsic binding constant is $K_i = 2.5 \times 10^4\ \text{M}^{-1}$. The BFc dendrimers were solubilized in water by complexation of the end groups with β-CD, resulting in large water-soluble supramolecular assemblies. Cyclic voltammetry (CV) and differential pulse voltammetry (DPV) showed that all the end groups are complexed to β-CD. Adsorption of the dendrimers at self-assembled monolayers (SAMs) of heptathioether-functionalized β-CD on gold ("molecular printboards") resulted in stable monolayers of the dendrimers due to the formation of multivalent host–guest interactions between the BFc end groups of the dendrimers and the immobilized β-CD molecules. The number of interacting end groups is 3, 4, and 4 for dendrimer generations 1, 2, and 3, respectively. The complexation of BFc to β-CD is sensitive to the oxidation state of the BFc unit. Oxidation of neutral BFc-$Fe_2^{(II,II)}$ to the cationic, mixed-valence biferrocenium BFc-$Fe_2^{(II,III)+}$ resulted in dissociation of the host–guest complexes. Scan-rate-dependent CV and DPV analyses of the dendrimer–β-CD assemblies immobilized at the β-CD host surface and in solution revealed that the dendrimers are oxidized in three steps. First, the surface-β-CD-bound BFc moieties are oxidized to the mixed-valence state, $Fe_2^{(II,III)+}$, followed by the oxidation of the non-surface-interacting BFc groups to the $Fe_2^{(II,III)+}$ state. The third step involves the oxidation of all the BFc moieties to the $Fe_2^{(III,III)2+}$ state.

Keywords: biferrocene · dendrimers · host–guest systems · mixed-valent compounds · self-assembly

Introduction

The immobilization of (bio)molecules that respond to external stimuli is of interest in, for instance, molecular electronics,[1] biochips,[2] and solar cells,[3] and for conducting single-molecule experiments.[4] Anchoring of molecules at surfaces is usually achieved by covalent attachment, by chemisorption, or by physisorption. These strategies of surface modification have the disadvantage that covalent modification is usually irreversible while chemi- and physisorption are thermodynamically and kinetically difficult to control. Recently, we described the immobilization of molecules by means of supramolecular interactions at so-called "molecular printboards".[5] Molecular printboards are self-assembled monolayers (SAMs) of host molecules to which guest molecules can bind.[5–7] We designed molecular printboards based on SAMs on gold of heptathioether-functionalized β-cyclodextrin (β-CD),[8] which forms well-ordered and densely packed monolayers. We also prepared molecular printboards on glass.[9] Onto these SAMs a variety of mono- and multivalent guest molecules were immobilized either by adsorption from solution or by microcontact printing (μCP) or dip-pen nanolithography (DPN) with submicron resolution.[6,7] The strength of the interaction between guest and host could be increased by using multivalent rather than monovalent interactions.[10,11] Indeed, we found that in μCP and DPN, multi-

[a] C. A. Nijhuis, K. A. Dolatowska, Dr. B. J. Ravoo, Prof. Dr. D. N. Reinhoudt
Supramolecular Chemistry and Technology
MESA+ Institute for Nanotechnology, University of Twente
P.O. Box 217, 7500 AE Enschede (The Netherlands)
Fax: (+31) 53-489-4645
E-mail: b.j.ravoo@utwente.nl
d.n.reinhoudt@utwente.nl

[b] Prof. Dr. J. Huskens
Molecular Nanofabrication
MESA+ Institute for Nanotechnology, University of Twente
P.O. Box 217, 7500 AE Enschede (The Netherlands)

ple supramolecular interactions between guest molecules and the β-CD host surface enhanced the pattern stability dramatically.[6,7]

Dendrimers are polyfunctional molecules of which the precise number of end groups is known for each generation. In addition, the end groups are located at the periphery of the molecule. Dendrimers have been used in various applications, such as in nanocontainers to encapsulate small guest molecules,[12] layer-by-layer assembly,[13] nanoreactors,[14] molecular recognition,[15] drug carriers,[16] catalysis,[17] and in nanofabrication.[18] Recently, we reported the patterned immobilization of adamantyl (Ad)-functionalized poly(propylene imine) (PPI) dendrimer guest molecules by supramolecular μCP.[7] To demonstrate that supramolecular interactions serve as an excellent tool to *control* binding to the molecular printboard by means of external stimuli, ferrocenyl (Fc)-functionalized dendrimers were adsorbed at the molecular printboard.[19] It is well known that Fc is able to form inclusion complexes with β-CD in aqueous media and that the complexation is strongly diminished upon electrochemical conversion of Fc to the ferrocenium cation.[20] Consequently, the binding of Fc-functionalized PPI dendrimers to β-CD SAMs can be completely controlled by electrochemistry, even in the case of the G5-PPI dendrimer with 64 Fc end groups and seven interactions with the host surface.[21]

Organometallic polymers and dendrimers based on Fc or Fc conjugates may find applications in a variety of fields owing to their reversible redox properties.[22] Conjugated Fc units are of special interest since mixed-valence states are accessible with noticeable electron mobilities and interesting electrical, redox, and magnetic properties.[23] The degree of electrochemical interaction between the conjugated Fc units is normally expressed as the difference in the redox potentials of the interacting units. Electronically communicating Fc units, linked for instance via a bridging silicon[24] or nitrogen atom[25] or via alkene or alkyne tethers,[26] have an oxidation potential difference (ΔE_p) in the range of 10–180 mV, depending largely on the length of the tether and the degree of conjugation. Directly linked Fc oligomers, like biferrocene (BFc), have electronically strong interacting metal centers with values of ΔE_p in the range of 240–300 mV.[22,23,26] The BFc groups can selectively be oxidized by I_2 to yield mixed-valence $Fe_2^{(II,III)+}$ complexes.[27] BFc moieties have been immobilized on gold nanoparticles and surfaces[28] and used to complex alkali and alkaline earth metal ions.[29]

In view of the interesting properties of BFc and its promising potential in organic electronics, we have investigated the possibilities of confining BFcs at a molecular printboard. PPI dendrimers of generation 1, 2, and 3 terminated with 4, 8, and 16 BFc moieties, respectively, were prepared. The ability of BFc to form inclusion complexes with β-CD was studied by using isothermal titration microcalorimetry (ITC). The adsorption of water-soluble dendrimer–β-CD assemblies at β-CD SAMs on gold was studied by using surface plasmon resonance (SPR) spectroscopy. The number of host–guest interactions for each dendrimer was investigated by electrochemical methods and SPR titrations. The BFc moiety can exist in three oxidation states, that is, the neutral $Fe_2^{(II,II)}$, the cationic $Fe_2^{(II,III)+}$, and the dicationic $Fe_2^{(III,III)2+}$ states. The redox processes, which control the ability of the dendrimers to form inclusion complexes with β-CD, were investigated by means of cyclic voltammetry (CV) and differential pulse voltammetry (DPV) analyses.

Results and Discussion

Synthesis: Three generations of BFc-terminated PPI dendrimers were prepared as outlined in Scheme 1. Ferrocene (**1**) was converted in situ into acetylmercurioferrocene, which, after reaction with LiCl, gave the chloromercurioferrocene (**2**), which could be easily separated from the disubstituted product. Subsequent reaction with *N*-iodosuccinimide gave the monofunctionalized iodoferrocene (**3**).[30] Ullmann coupling gave BFc (**4**).[31] Friedel–Craft acylation with succinic anhydride gave the monoacylated product **5** in moderate yields (32%) and, subsequently, the carboxylic acid **5** was converted into the more reactive ester **6**. The BFc-decorated PPI dendrimers **7a**–**7c** were obtained in 69–95%

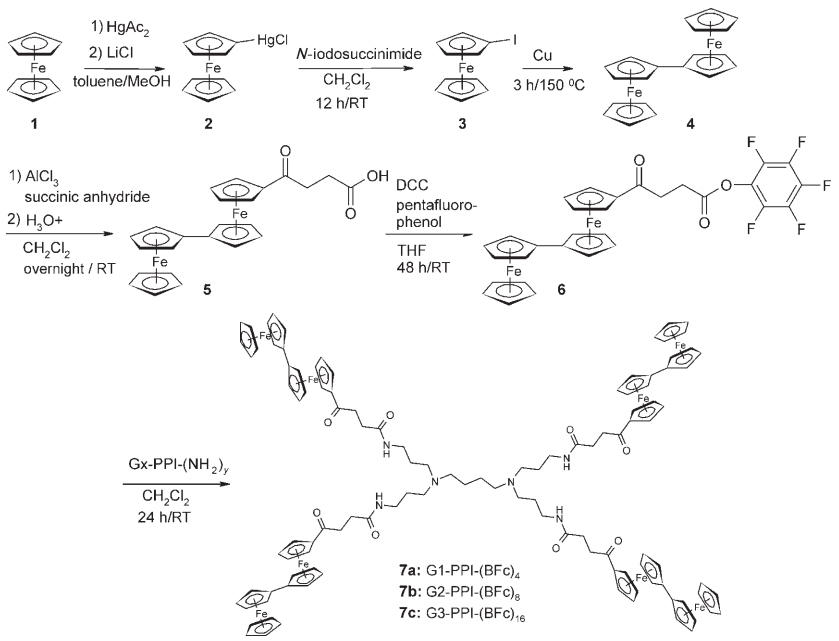

Scheme 1. Synthesis of biferrocenyl (BFc)-functionalized dendrimers.

yields by reaction of **6** with the corresponding amino-terminated PPI dendrimers, G1-PPI-$(NH_2)_4$, G2-PPI-$(NH_2)_8$, or G3-PPI-$(NH_2)_{16}$. All BFc dendrimers and intermediates were characterized by using ^1H and ^{13}C NMR spectroscopy, elemental analysis, and mass spectrometry. All the analytical data were consistent with the molecular structures.

BFc–β-CD complexation: The BFc carboxylic acid **5** is quite soluble in water at high pH and its complexation to β-CD was studied by means of ITC. Figure 1 shows the exothermic heat profile versus the molar ratio [β-CD]/[**5**] obtained by titration of a solution of β-CD against a solution of **5**. The inflection point is very close to a molar ratio of 1:1 and thus the data were fitted to a model for a 1:1 interaction of the BFc guest with the β-CD host. The intrinsic binding constant K_i and the enthalpy $\Delta H^\ominus$ of complexation are $K_i = 2.5\times10^4\,\text{M}^{-1}$ and $\Delta H^\ominus = -8.5\,\text{kcal mol}^{-1}$, respectively. A rather large unfavorable entropic term was found ($T\Delta S^\ominus = -2.7\,\text{kcal mol}^{-1}$), indicating that the formation of the BFc–β-CD complex is enthalpy driven. Typical K values for Fc derivatives are one order of magnitude smaller: for ferrocenecarboxylate $K_i = 2.1\times10^3\,\text{M}^{-1}$, $\Delta H^\ominus = -3.6\,\text{kcal mol}^{-1}$, and $T\Delta S^\ominus = 0.9\,\text{kcal mol}^{-1}$, and for ferrocene quaternary ammonium salts K_i values ranging from 7.1×10^2 to $4.8\times10^4\,\text{M}^{-1}$, $\Delta H^\ominus$ values ranging from -5.1 to $-6.8\,\text{kcal mol}^{-1}$ and $T\Delta S^\ominus$ values ranging from -0.5 to $-2.1\,\text{kcal mol}^{-1}$ have been reported.[32] Ferrocenemethanol gave a comparable binding constant of $9.9\times10^3\,\text{M}^{-1}$, but with a less favorable $\Delta H^\ominus$ value of $-6.1\,\text{kcal mol}^{-1}$ and a more favorable $T\Delta S^\ominus$ value of $-0.7\,\text{kcal mol}^{-1}$.[33] The large difference in $\Delta H^\ominus$ for BFc relative to Fc can be explained by the so-called "expanded hydrophobic surface", which has been proposed to explain trends observed for the inclusion of guests with an increasing number of aliphatic carbon atoms (N_c).[32] Guest molecules with an increasing N_c give more negative $\Delta G^\ominus$ and $\Delta H^\ominus$ values while $\Delta G/N_c$ and $\Delta H/N_c$ remains constant. This can be rationalized by considering that in the case of longer chain lengths at least one methylene group is forced to stay outside the hydrophobic cavity and, hence, increases the exposed hydrophobic surface. Upon complexation of a guest that is only partly included, water molecules surrounding the complex must solvate part of the guest. Both the release of water molecules from the cavity and the rearrangement of water molecules play a crucial role in the unfavorable complexation entropy of BFc relative to ferrocenemethanol. The BFc moiety is much larger than the Fc moiety and, therefore, β-CD cannot accommodate a BFc moiety as well as it can a Fc moiety. This results in a more negative $\Delta H^\ominus$ by $2.4\,\text{kcal mol}^{-1}$ relative to Fc that is only partly compensated by an unfavorable $T\Delta S^\ominus$, resulting in a high K_i for BFc relative to Fc guests.

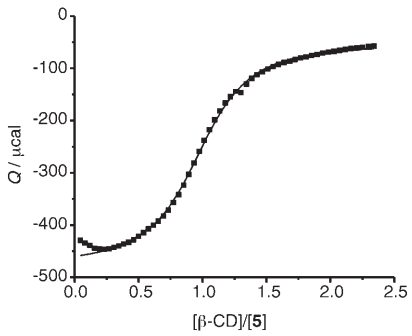

Figure 1. Heat evolved per injection plotted versus the molar ratio [β-CD]/[**5**] (■: experimental data; solid line: fit) for the calorimetric titration of 10 mM β-CD with 1 mM **5** in water at pH 12 (NaOH) at 295 K.

Dendrimer–β-CD assemblies: The apolar BFc dendrimers are virtually insoluble in water, but at pH 2 the addition of β-CD (β-CD/BFc = 10) resulted in soluble dendrimer–β-CD assemblies. Owing to the mutual repulsion of the protonated amines the dendrimers expand into their most extended conformation and, for this reason, β-CD readily forms inclusion complexes with all the BFc end groups of the dendrimers. All dendrimers could be solubilized in water after prolonged ultrasonication.[34] The dendrimer–β-CD assembly **7b**·$(\beta\text{-CD})_8$ is depicted schematically in Scheme 2.

The solubilities of the BFc dendrimer–β-CD assemblies are low relative to the solubilities of the ferrocenyl (Fc) or adamantyl (Ad) analogues.[19,34] G1-PPI-$(BFc)_4$ is relatively soluble and solutions of up to 1–2 mM (BFc equivalent) could be prepared at pH 2 in the presence of excess β-CD. The solubility decreased with increasing generation, for example, solutions of G2-PPI-$(BFc)_8$ up to about 0.5 mM (BFc equivalent) could be prepared, while G3-PPI-$(BFc)_{16}$ was only soluble up to 0.2 mM BFc equivalent. In comparison, solutions of the Fc and Ad dendritic analogues of typically 10 mM in functionality could be prepared for all generations. The BFc complexes are less soluble than the Fc and Ad complexes because the large BFc group is shielded less efficiently by the β-CD cavity.

The BFc dendrimer–β-CD assemblies were characterized by means of CV and DPV analyses. The two oxidation waves observed correspond to the oxidation of both metal centers in a two-step one-electron redox process (Figure 2). Upon oxidation of the first metal center at $E_{p,1} = 50$ mV, the BFc moiety changes from a neutral $Fe_2^{(II,II)}$ complex to a positively charged mixed-valence state $Fe_2^{(II,III)+}$. The second oxidation at $E_{p,2} = 350$ mV results in a dicationic $Fe_2^{(III,III)2+}$ complex. The large difference in oxidation potential ΔE_p of 300 mV indicates that the metal centers communicate strongly electrochemically. This is consistent with values reported for other BFc derivatives.[22,23,26] The comproportionation constant K_{com} of 1.2×10^5 was calculated using ΔE_p according to $K_{com} = e^{-(RT/F)\Delta E_p}$. The value of K_{com} suggests that the BFc dendrimers belong to Class II of the Robin–Day classification.[35] This classification implies that there is some, but not complete, charge delocalization in the mixed-valence state and that the charge resides mostly at the most electron-rich metal center, that is, the terminal Fc.

All end groups undergo oxidation and reduction at the same potentials indicating that all end groups are identical

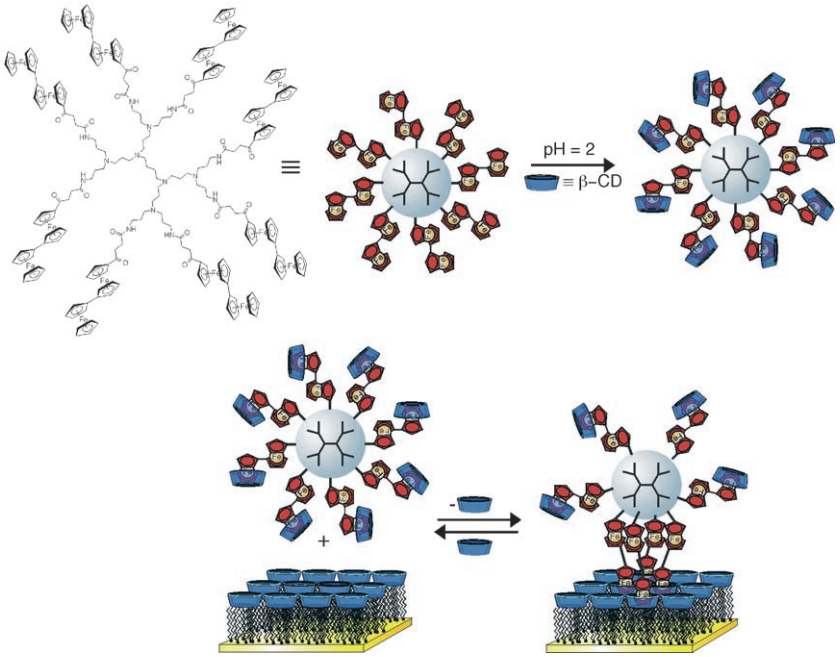

Scheme 2. Top: Second-generation biferrocenyl dendrimer G2-PPI-$(BFc)_8$ (**7b**) and its formation with β-CD of water-soluble assemblies. Bottom: The adsorption of the dendrimer–β-CD assembly at a β-CD SAM ("molecular printboard").

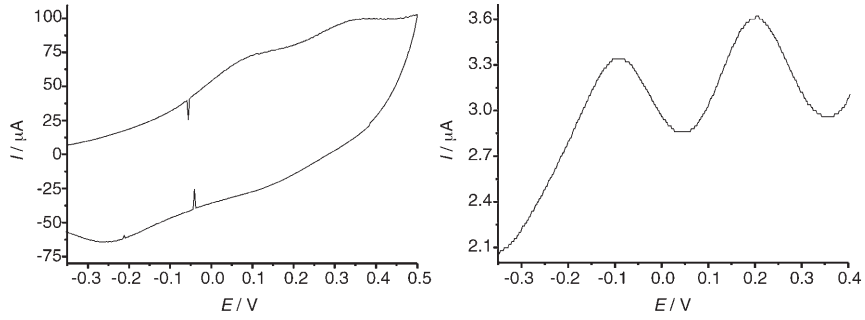

Figure 2. Left: CV of the G1-PPI-$(BFc)_4$–β-CD assembly at a bare gold electrode (1 mM in BFc functionality) in the presence of 10 mM β-CD and 0.1 M NaCl; pH 2, scan rate = 1 $V s^{-1}$. Right: DPV of the same solution; scan rate = 1 $mV s^{-1}$.

and interact with β-CD in solution. It is well known that all redox end groups of dendrimers (even for large dendrimers containing hundreds of end groups) behave independently and are oxidized at the same potential.[36] Besides normal electron-transfer pathways (for instance, an electron-hopping mechanism), another mechanism has been proposed for dendrimers that is based on their rotational diffusion.[37] Therefore, it can safely be assumed that all end groups of the BFc dendrimers in this study are redox active.

SPR spectroscopy of BFc dendrimers on the molecular printboard: The BFc dendrimers were adsorbed at the β-CD host surface from aqueous solutions of the dendrimer–β-CD assemblies (Scheme 2). The dendrimers bind strongly to the printboard owing to the high effective concentration of host sites at the surface and the high local concentration of guest groups at the periphery of the dendrimers. The dendrimers readily form densely packed monolayers at the host surface for a number of reasons: 1) the individual host–guest interactions are by nature reversible, 2) the PPI dendrimers are flexible and can extend as much as is sterically allowed to access the maximum number of β-CD sites at the surface, and 3) the multivalency principle prescribes that molecules will interact (under equilibrium conditions) with the maximal number of interactions p_b.[10]

The adsorptions and stabilities of the dendrimer–β-CD assemblies at the host surface with respect to competitive solutions were examined by using SPR spectroscopy.[38] The injection of guest molecules resulted in typical adsorption curves, as illustrated in Figure 3. Rinsing with a competitive solution of 10 mM aqueous β-CD at pH 2 after adsorption of G1-PPI-$(BFc)_4$ resulted in the desorption of most of the dendrimers from the surface (Figure 3A), whereas G2-PPI-$(BFc)_8$ (Figure 3B) and G3-PPI-$(BFc)_{16}$ (Figure 3C) could not be removed from the host surface even upon rinsing extensively. After rinsing with β-CD at pH 2 only a small decrease in the SPR sensogram was observed in the case of G2-PPI-$(BFc)_8$ and a second guest injection resulted in a small increase, but after washing again with 10 mM aqueous β-CD at pH 2 the signal decreased to a similar extent as before the second guest injection. These observations confirm that already after the first injection a densely packed monolayer of dendrimers had formed at the host surface. The small decrease in the SPR signal upon rinsing after guest injection indicates removal of nonspecifically bound guest molecules. In addition, in the case of G2-PPI-$(BFc)_8$ a small but steady decrease in the SPR signal was observed during rinsing. This decrease implies that the G2-PPI-$(BFc)_8$ serves as an intermediate case in terms of stability as G1-PPI-$(BFc)_4$ can be removed completely and G3-PPI-$(BFc)_{16}$ cannot be removed at all from the surface.

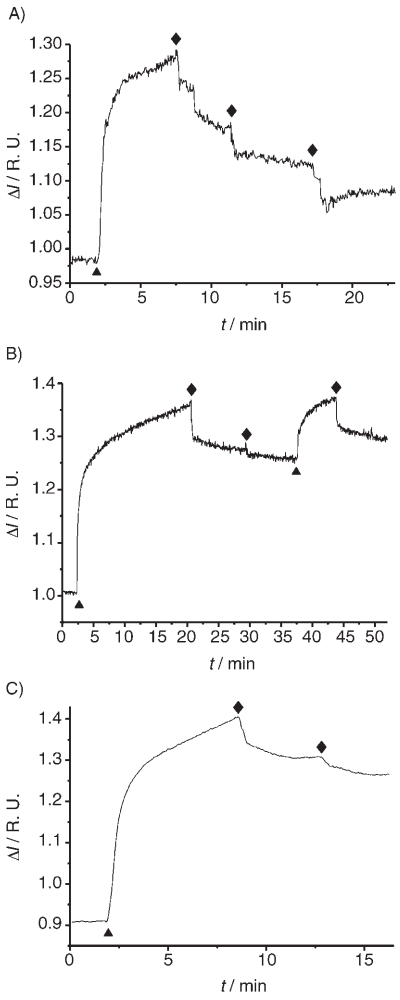

Figure 3. SPR sensogram of A) G1-PPI-$(BFc)_4$ (**7a**), B) G2-PPI-$(BFc)_8$ (**7b**), and C) G3-PPI-$(BFc)_{16}$ (**7c**) adsorption at a β-CD SAM. ▲ = injection of guest ([**7a**] = 50 μM, [**7b**] = 13 μM, and [**7c**] = 6.3 μM) in 10 mM β-CD; ◆ = wash with an aqueous solution of 10 mM β-CD at pH 2. (R.U. = reflectivity unit.)

The two larger dendrimers have sufficient BFc–β-CD interactions to form kinetically stable assemblies at the β-CD surface at room temperature.

The number of interactions p_b of the dendrimers with the β-CD host surface can be determined from SPR titrations of aqueous solutions of dendrimer–β-CD assemblies against the host surface. The changes in SPR signal due to the adsorption of guest as a function of guest concentration can be fitted to a surface binding model for multivalent host–guest interactions.[10] This model is based on the assumption that all BFc–β-CD interactions are independent and equivalent in solution and at the surface. The model interprets multivalent interactions in terms of the high effective concentration C_{eff} of available host molecules at the surface upon binding of the first guest group of the dendrimer and accounts for the free binding sites of the dendrimer as well as for the competitive interaction with β-CD in solution. Previously, we showed that for small, monovalent guests the intrinsic binding constant at the surface $K_{i,s}$ is close to the intrinsic binding constant in solution $K_{i,l}$.[39,40] To investigate if this also holds for BFc, titrations of **5** (aqueous solution at pH 12) against the β-CD SAM were performed and monitored by using SPR spectroscopy. Figure 4 shows the binding data and the fit to the Langmuir isotherm. From the isotherm, we obtained a binding constant $K_i = 2.2 \times 10^4\,M^{-1}$, which indeed is very similar to the binding constant in solution obtained by using ITC.

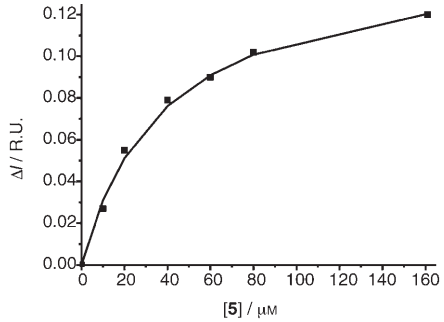

Figure 4. SPR titration curve of **5** (aqueous solution at pH 12) against a β-CD SAM and the fit to a Langmuir isotherm. (R.U. = reflectivity unit.)

The BFc dendrimers interact with the surface with the maximum number of interactions because the effective concentration C_{eff} of β-CD hosts at the surface (0.3 M) is much larger than the concentration of β-CD in solution. The binding curve for the dendrimers can be fitted by optimizing $K_{i,s}$ for various p_b values, but only those fits that give plausible $K_{i,s}$ values, that is, $K_{i,s} \approx K_{i,l}$, will correspond to the real p_b value.[19] Titrations were performed with G1-PPI-$(BFc)_4$ using a competitive solution (10 mM β-CD at pH 2), as the other two dendrimers form kinetically stable assemblies. Figure 5 shows a typical titration curve and in Table 1 the fitting solutions are given for $p_b = 2$, 3, and 4. Figure 5 also shows a fit that was found assuming three interactions with the surface per molecule ($p_b = 3$). An intrinsic binding constant $K_{i,s}$ at the surface of $2.1 \times 10^4\,M^{-1}$ per BFc–β-CD interaction was obtained in this case, which compares very well

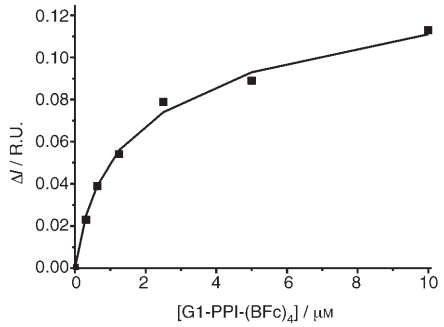

Figure 5. SPR titration curve of G1-PPI-$(Fc)_4$ (**7a**) with 10 mM β-CD at pH 2 against a β-CD SAM with a fit for three interactions. (R.U. = reflectivity unit.)

Table 1. Optimized $K_{i,s}$ values for SPR titrations of G1-PPI-$(BFc)_4$ (**7a**) against β-CD SAMs.

Number of interactions p_b	$K_{i,s}$ [M^{-1}][a]	SPR max[a]	R
2	1.3×10^5	0.33	0.98
3	2.1×10^4	0.56	0.98
4	9.4×10^3	1.0	0.98

[a] Determined using the multivalency model[10] with $C_{eff,max}=0.3$ M and $K_{i,1}=2.5\times10^4\,M^{-1}$ for varying p_b.

with $K_{i,1}=2.5\times10^4\,M^{-1}$. In contrast, for p_b values of 2 and 4, only implausible $K_{i,s}$ values were found (Table 1).

This observation agrees very well with our previous complexation study of Fc dendrimers of various types and generations.[21] The stabilities of such assemblies increase with increasing generation. It was also found that five Fc–β-CD ($p_b=5$) interactions invariably resulted in kinetically stable assemblies at the β-CD host surface. Four interactions ($p_b=4$) resulted in kinetically stable assemblies provided that the spacer length between the different end groups was short or (in equilibrating assemblies) the spacer groups were long. In comparison with the Fc dendrimers, the BFc dendrimers have a small dendritic core with short tethers between the end groups and the dendritic core and a higher $K_{i,s}$ and thus are expected to give kinetically stable assemblies at $p_b\geq4$.

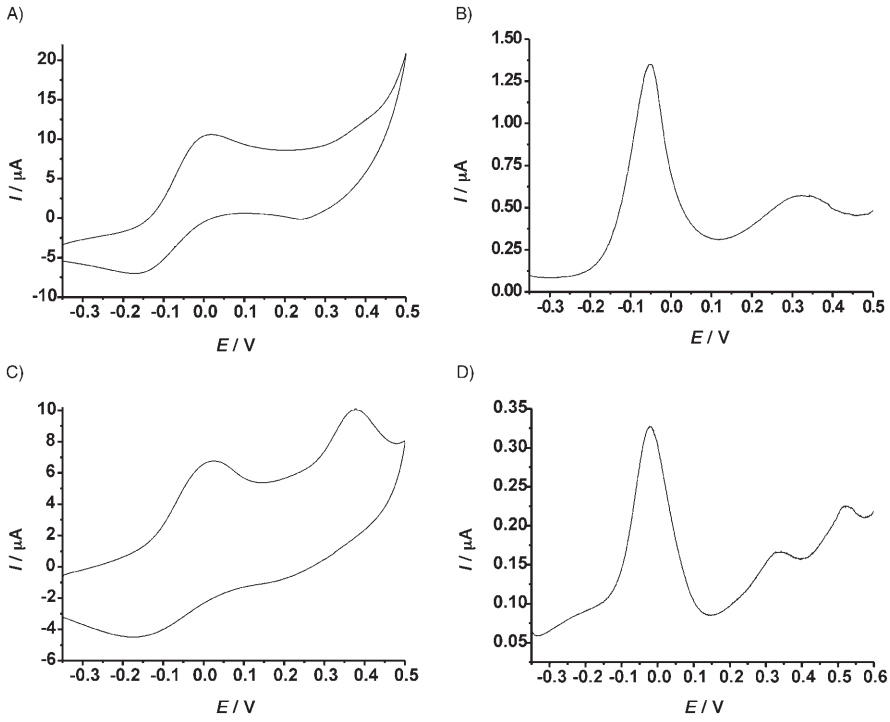

Figure 6. CV (A: scan rate = 100 mV s^{-1} and C: scan rate = 20 mV s^{-1}) and DPV (B and D) of a 1 mM (in functionality) aqueous solution of A,B) G1-PPI-$(BFc)_4$ (**7a**) and C,D) G3-PPI-$(BFc)_{16}$ (**7c**) with 10 mM β-CD at pH 2 at gold electrodes covered with a β-CD SAM.

Electrochemistry of BFc dendrimers on the molecular printboard: CV and DPV analyses of the BFc dendrimer–β-CD assemblies at bare gold electrodes showed two oxidation waves of similar intensity (Figure 2). In contrast, CV analysis of the G1-PPI-$(BFc)_4$–β-CD assembly at a gold electrode modified with a β-CD SAM showed a pronounced first wave while the second oxidation wave is hardly visible (Figure 6A). The DP voltammograms clearly showed the second oxidation wave of the assemblies at the host surface in the case of G1-PPI-$(BFc)_4$–β-CD (Figure 6B). Again the first signal is intense and sharp, while the second is very broad and significantly less pronounced. These observations can be explained by the hypothesis that a single oxidation diminishes the BFc–β-CD interaction because of the charge delocalization over the BFc moiety. The most electron-rich metal center is the terminal Fc (i.e., the Fc without the electron-withdrawing carbonyl linker), implying that the part of the BFc moiety complexed to the β-CD is (more) positively charged in the mixed-valence state. This suggests that oxidation of one iron center in the BFc leads to desorption of the dendrimers from the host surface and, therefore, a second oxidation is more difficult. This scenario is supported by the shifts of both oxidation potentials in comparison with the experiments performed at bare gold electrodes (Figure 2). $E_{p,a,1}$ is shifted by 40 mV to higher oxidation potentials in the presence of the β-CD SAM, while $E_{p,a,2}$ is shifted by 120 mV to higher potentials, leading to a large ΔE_p value of 374 mV, compared with $\Delta E_p=301$ mV at bare gold electrodes.

Similar behavior was observed for G2-PPI-$(BFc)_8$ (not shown) and G3-PPI-$(BFc)_{16}$. However, for G3-PPI-$(BFc)_{16}$ a second oxidation wave was clearly visible in the cyclic voltammogram recorded under the same conditions (Figure 6C). In addition, the DP voltammograms of both G2-PPI-$(BFc)_8$ (not shown) and G3-PPI-$(BFc)_{16}$ (Figure 6D) revealed the presence of a third wave at 490 and 501 mV, respectively. This suggests a complicated oxidation mechanism due to the host–guest chemistry of the dendrimers and the molecular printboard involving a three-step oxidation process of the molecules at the host surface. A possible explanation is outlined in Scheme 3. During the first step ($E_p=-24$ mV) the interacting BFc moieties are oxidized resulting in partially oxidized dendrimers that interact weakly with the β-CD SAM. Subsequently, the noninteracting groups are oxidized ($E_p=-340$ mV) and finally all end groups undergo

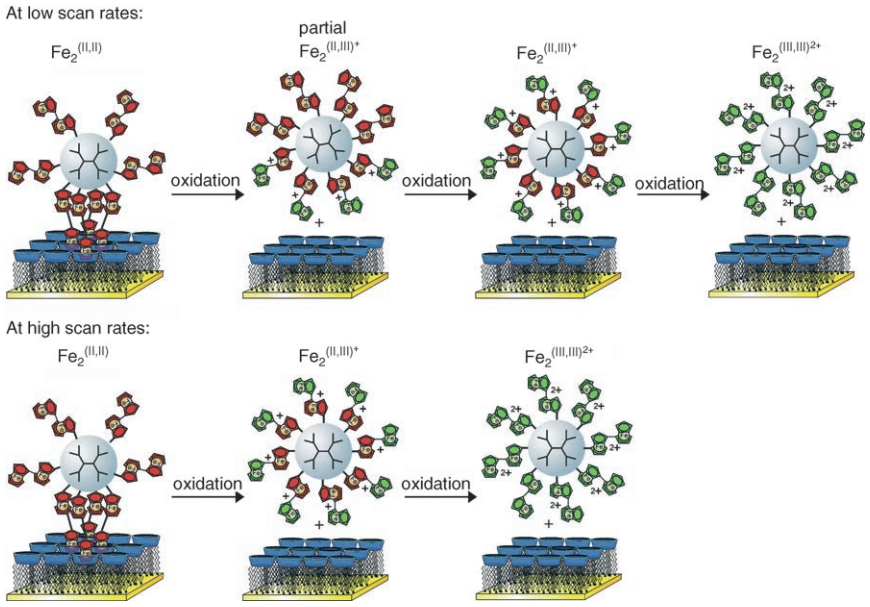

Scheme 3. Schematic of the proposed oxidation mechanism of biferrocenyl dendrimers in solution and immobilized at the β-CD host surface, outlined for G2-PPI-$(BFc)_8$, which has four interactions with the host surface (see text). The proposed sequences of oxidation and desorption are scan-rate-dependent.

a second oxidation ($E_p = 520$ mV). More details and evidence in support of this proposed mechanism are discussed below.

The G3-PPI-$(BFc)_{16}$–β-CD assemblies have a ΔE_p value of 352 mV and G2-PPI-$(BFc)_8$ has a ΔE_p value of 360 mV. The increase in ΔE_p at the host surface is caused by the fact that the dendrimers have a strong interaction with the host surface. The interaction of the mixed-valence state dendrimers (with all moieties in the $Fe_2^{(II,III)+}$ state) may not be entirely negligible. The interaction of these species can be estimated from Equations (1) and (2), in which K_i, $K_{1,1}$, and $K_{1,2}$ are the equilibrium constants for BFc binding to β-CD, with BFc in the $Fe_2^{(II,II)}$, partial $Fe_2^{(II,III)+}$, and $Fe_2^{(II,III)+}$ states, respectively.[41]

$$\Delta\Delta E_{p,1} = E_{p,2} - E_{p,1} = (RT/F)\ln(K_i/K_{1,1}) \quad (1)$$

$$\Delta\Delta E_{p,2} = E_{p,3} - E_{p,2} = (RT/F)\ln(K_{1,1}/K_{1,2}) \quad (2)$$

These equations hold if the system is reversible and if [β-CD] ≫ [BFc]. These conditions are met when the scan rates are low and [BFc] = 0.1 mM and [β-CD] = 10 mM. $K_i = 2.5 \times 10^4\,M^{-1}$ and the difference in ΔE_p leading to $\Delta\Delta E_{p,1}$ and $\Delta\Delta E_{p,2}$ for the second and third oxidation waves gives $K_{1,1}$ and $K_{1,2}$ at bare gold electrodes and the β-CD SAM decorated electrodes, respectively. For the partially oxidized dendrimers, $\Delta\Delta E_{p,1}$ values of 73, 69, and 52 mV for G1-PPI-$(BFc)_4$, G2-PPI-$(BFc)_8$, and G3-PPI-$(BFc)_{16}$, respectively, were found resulting in $K_{1,1}$ values of 11, 20, and 117 M^{-1}. Thus, the assemblies have a small, but significant interaction with the host surface in the partial mixed-valence state. The third oxidation wave has a $\Delta\Delta E_{p,2}$ value of more than 200 mV which leads to $K_2 \ll 1\,M^{-1}$, indicating that the dendrimers in the $Fe_2^{(II,III)+}$ state do not have any significant interaction with the host surface.

To elucidate the complex redox behavior of the dendrimers at the host surface and to determine the number of interactions of all dendrimers, scan-rate-dependent CV analyses were performed on monolayers of the dendrimers at the host surface. The dendrimers were adsorbed at the β-CD host surface by immersion of the β-CD host monolayers[19] into aqueous solutions containing the BFc dendrimer–β-CD assemblies (Scheme 2), followed by rinsing with water and drying under a stream of nitrogen. The electrochemically induced desorption of the dendrimers from the molecular printboard is shown in Figure 7. In a typical experiment 10 successive CV scans were recorded at different substrates with the scan rate ν ranging from 5 mV s^{-1} to 10 V s^{-1}. As the potential increases to 50 mV, the BFc groups are oxidized and mixed-valence biferrocenium cations $Fe_2^{(II,III)+}$ are formed. The BFc $Fe_2^{(II,III)+}$ cations dissociate from the β-CD SAM and diffuse into the solution.

The electrochemically induced desorption of the BFc dendrimers is completely analogous to that of Fc dendrimers.[19] Only dendrimers that remain in close proximity to the surface may be reduced and rebind to the surface. During subsequent scans only rebound dendrimers are oxidized resulting in a rapid decrease of peak intensity. In fact, already after the first scan most dendrimers are removed from the surface at low ν as is shown in Figure 7A–C. By increasing ν to 5 V s^{-1}, as is shown for G3-PP-$(BFc)_{16}$ in Figure 7D, not all dendrimers have sufficient time to diffuse away from the host substrate and a significant fraction is reduced and readsorbed.

The numbers of interactions p_b were determined from the relative surface coverage of the surface-confined β-CD ($\Gamma_{\beta\text{-CD}}$) and BFc units (Γ_{BFc}). The Γ_{BFc} was determined from the CV data by integration of both oxidation waves of the first scan of the *i*–*E* curves, which gives the total charge Q_{tot}, and by using the relation $\Gamma_{BFc} = Q_{tot}/nFA$, in which n is the number of electrons per mole of reaction, F is the Faraday constant, and A is the surface area of the electrode.[42] We found that Q_{tot} is constant at ν ranging from 5 mV s^{-1} to 10 V s^{-1}, indicating surface-confined processes. The surface coverage of the β-CD adsorbate molecules $\Gamma_{\beta\text{-CD}}$ (8×10^{-11} mol cm^{-2}) was estimated from Corey–Pauling–Koltun (CPK) models, atomic force microscopy (AFM) studies,[8]

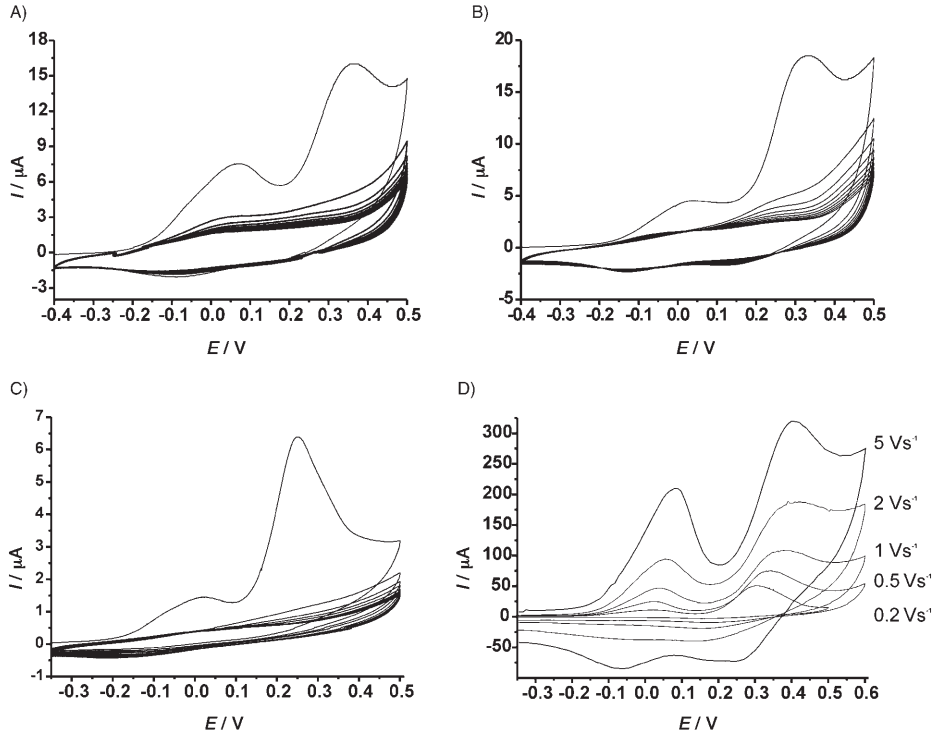

Figure 7. Electrochemical desorption from a β-CD SAM of A) G1-PPI-$(BFc)_4$ (**7a**) induced and observed by CV, scan rate = 200 mV s^{-1}, 0.1 M K_2SO_4, 10 scans; B) G2-PPI-$(BFc)_8$ (**7b**) at 100 mV s^{-1}, 0.1 M K_2SO_4, 10 scans; C) G3-PPI-$(BFc)_{16}$ (**7c**) at 25 mV s^{-1}, 0.1 M K_2SO_4, 10 scans. D) The first scan of similar desorption experiments at scan rates of 0.2, 0.5, 1, 2, and 5 V s^{-1} for G3-PPI-$(BFc)_{16}$.

and SPR measurements for a calixarene bis-adamantyl derivative.[39] As described before, the relative coverage $\Gamma_{\beta\text{-CD}}/\Gamma_{BFc}$ provides the number p_b of inclusion interactions per dendrimer molecule with the host surface by using $p_b = p_{tot}\Gamma_{\beta\text{-CD}}/\Gamma_{BFc}$, where p_{tot} is the total number of end groups.[10,19,21]

For G1-PPI-$(BFc)_4$, a $\Gamma_{\beta\text{-CD}}/\Gamma_{BFc}$ ratio of 0.77 was found, which implies that $p_b = 3$ and thus three BFc end groups (out of four) interact with the host surface. For G2-PPI-$(BFc)_8$ the $\Gamma_{\beta\text{-CD}}/\Gamma_{Fc}$ ratio is 0.55, which indicates $p_b = 4$ interactions (out of eight), and for G3-PPI-$(BFc)_{16}$ the ratio was 0.26 suggesting $p_b = 4$ interactions (out of 16). Two BFc moieties of the same branch are separated by 2.2 nm and, consequently, both may interact simultaneously with two β-CD molecules at the molecular printboard as the center-to-center spacing of two adjacent β-CD molecules at the surface is 2.1 nm.[8,19,21] However, two BFc groups of different branches are separated by 2.8 nm, implying that G1-PPI-$(BFc)_4$ can form only three interactions with the host surface, since to complex a fourth β-CD at the surface a distance of 3.5 nm has to be covered. The maximal distance of two BFc groups in G2-PPI-$(BFc)_8$ is 3.9 nm, which is sufficient for forming four interactions. Thus, the number of interactions found from electrochemical measurements corresponds very well with the estimated sizes of the molecules compared with the lattice periodicity of the molecular printboard. The number of interactions in the first generation is in full agreement with the SPR results. The maximal distance between two end groups in G3-PPI-$(BFc)_{16}$ is 5.3 nm, indicating that seven or eight interactions would have been possible, but the number of interactions of G3-PPI-$(BFc)_{16}$ is only four due to steric hindrance since the dendritic core is relatively small. In comparison, G3-PPI-$(Fc)_{16}$ lacks the tether and forms four interactions.[21] This indicates that the small tether between the dendritic core and the BFc moiety is not sufficient to overcome the steric hindrance and to increase the number of interactions.

The surface areas of the two waves of the first scan are different and the ratio of the charge of the first Q_1 and the second wave Q_2 is dependent on the dendrimer generation (Figure 7A–C) as well as on the scan rate ϑ (Figure 7D). In all cases Q_1 was smaller than Q_2 at low ϑ. The Q_1/Q_2 ratio was 0.63 for G1-PPI-$(BFc)_4$, 0.33 for G2-PPI-$(BFc)_8$, and 0.14 for G3-PPI-$(BFc)_{16}$. The same three-step oxidation mechanism that was proposed to explain the CV and DPV data for the solution experiments can also be used here. During the first oxidation only the iron center of the BFc end groups interacting with the surface are oxidized, while during the second oxidation the remaining metal centers of the entire dendrimer are oxidized, as is outlined in Scheme 3. This implies that in the case of G1-PPI-$(BFc)_4$, which has three interactions, during the first oxidation step, three metal centers are oxidized, whereas during the second oxidation step the remaining five metal centers are oxidized leading to a ratio of Q_1/Q_2 of 0.60 (3/5). For G2-PPI-$(BFc)_8$ with 16 iron centers and four interactions the ratio is 0.33 (4/12) and for G3-PPI-$(BFc)_{16}$ with 32 iron centers and four interactions the theoretical ratio is 0.14 (4/28). The theoretical Q_1/Q_2 ratios compare very well with the measured ratios.

We observed that increasing ϑ led to an increase of the Q_1/Q_2 ratios until at high ϑ the Q_1/Q_2 ratio increased to a maximum of 1 and remained constant for all dendrimers. This is illustrated in Figure 7D for G3-PPI-$(BFc)_{16}$ at ϑ values ranging from 0.2 to 5 V s^{-1} and in Figure 8 in which the Q_1/Q_2 ratios for G3-PPI-$(BFc)_{16}$ are plotted versus ϑ for ϑ ranging from 5 mV s^{-1} to 10 V s^{-1}. Additionally, in Figure 8 the linear dependency of the Q_1/Q_2 ratio on ϑ is shown between 50 mV s^{-1} and 2 V s^{-1}. The other dendrimers behaved in the same way.

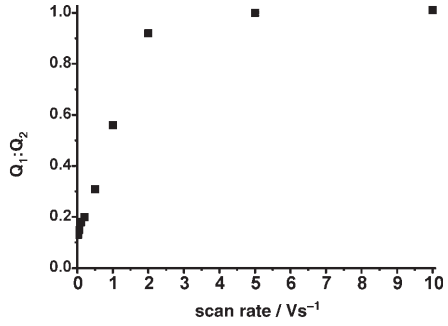

Figure 8. Scan-rate dependency of the Q_1/Q_2 ratio for G3-PPI-$(BFc)_{16}$ adsorbed at the host surface: determined at scan rates of 0.005, 0.010, 0.025, 0.05, 0.1, 0.2, 0.5, 1, 2, 5, and 10 Vs^{-1}.

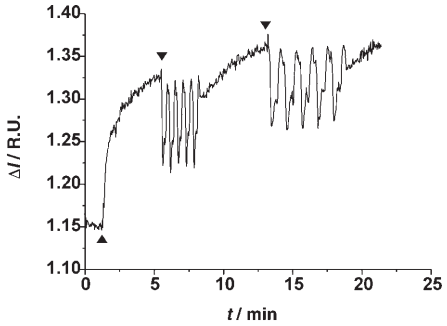

Figure 9. SPR response during five CV scans of a 0.25 mM solution of G1-BFc-$(Fc)_4$ at a β-CD SAM with 10 mM β-CD at pH 2. ▲ = injection of a 0.25 mM solution of G1-BFc-$(Fc)_4$ with 10 mM β-CD at pH 2; ▼ = five CV scans at 50 (left) and 25 mVs^{-1} (right). (R.U. = reflectivity unit.)

These observations support the oxidation process illustrated in Scheme 3. The redox mechanism for the oxidation of the BFc dendrimers adsorbed at the surface is a two-step single-electron redox process for all end groups, but the potential at which the surface-bound end groups undergo the first oxidation is lower than that for the noninteracting moieties. The oxidation potential of the noninteracting groups is almost the same as that at which the second metal center of the BFc moieties are oxidized (Scheme 3, upper part). At very low scan rates, for example, 1 mVs^{-1} or lower, a shoulder is observed on the second oxidation wave. The dissociation of the BFc–β-CD inclusion complexes is fast relative to the electrochemical timescale at low ϑ, but becomes comparable at intermediate ϑ. Therefore, the Q_1/Q_2 ratio gradually increases by increasing ϑ linearly, which is a characteristic of a surface-confined process. (For diffusion-dependent processes, there is a square-root relationship.) At high ϑ the dissociation is slow on the electrochemical timescale and all BFc end groups undergo oxidation to the mixed-valence state at the same potential to give $Q_1 = Q_2$ (Scheme 3, lower part). This interpretation is consistent with the CV and DPV experiments of the dendrimer–β-CD assemblies at the β-CD SAM at which DPV showed three distinct oxidation waves. The increase in the observed $K_{1,2}$ values with increasing generation can be rationalized by the increase in the number of noninteracting end groups, for example, 1, 4, and 12 for generation 1, 2, and 3, respectively.

Electrochemistry and SPR spectroscopy combined: In order to prove unambiguously that oxidation of one iron center of the BFc units leads to dissociation of the BFc–β-CD host–guest complex and consequent desorption of the dendrimers from the host surface, CV was performed in combination with SPR spectroscopy (Figure 9).[43] Combining these two techniques gives crucial information about the efficiency and the desorption rate of the dendrimers upon electrochemical oxidation, since the electrochemical timescale can be coupled to the SPR timescale. The experiments were performed in stationary solutions, that is, the dendrimer–β-CD assemblies were present in solution and at the β-CD SAM because under these conditions the adsorption and desorption processes are limited by diffusion. A solution of G1-PPI-$(BFc)_4$ was added to a β-CD SAM (1 mM solution in functionality in the presence of 10 mM β-CD at pH 2) and a typical adsorption curve was observed, as described above in the SPR section. Five successive CV scans were applied at scan rates of 50 and 25 mVs^{-1} and at potentials just below the first cathodic peak potential $E_{p,c,1}$ the dendrimers desorbed from the monolayer slowly, but just above $E_{p,c,1}$ virtually all dendrimers were removed. At this potential the BFc units are in the mixed-valence state $Fe_2^{(II,III)+}$ confirming unequivocally that the oxidation of one metal center dramatically diminishes the BFc–β-CD interaction. The SPR signal did not change upon increasing the potential well above $E_{p,c,1}$ and above the second oxidation potential $E_{p,c,2}$, because any dendrimer binding to the surface from solution would directly be oxidized. When the potential (during the backward scan) reached the first anodic peak potential $E_{p,a,1}$, the dendrimers started to adsorb again at the β-CD SAM, which is apparent from the characteristic adsorption curve in the SPR response. At potentials below $E_{p,a,1}$ the adsorbed dendrimers were not oxidized. During subsequent scans the dendrimers continued to adsorb at the host surface until $E_{p,c,1}$. This cycle of adsorption and desorption was repeated and all CV scans caused the same increase in SPR response between reduction and oxidation, and decrease between oxidation and reduction. Since stationary conditions were used the degree of monolayer formation of the dendrimers at the β-CD SAM is only dependent on the scan rate ϑ. Lower scan rates increase the time between reduction and oxidation in successive scans, for example, $E_{p,a,1}$ and $E_{p,c,1}$, and thus the adsorption and desorption times of the dendrimers.

Conclusion

A new type of dendrimer functionalized with electrochemically communicating BFc end groups has been prepared. BFc carboxylate **5** readily forms stable inclusion complexes with β-CD and the binding constant is $2.5 \times 10^4\ M^{-1}$, which is an order of magnitude larger than that of Fc–β-CD complexes. The higher complexation constant is caused by a fa-

vorable $\Delta H^{\ominus}$ value. SPR titrations showed that BFc also forms inclusion complexes with β-CD SAMs with a binding constant similar to that found in solution. Three generations of BFc dendrimers could be dissolved in water in the presence of β-CD. β-CD complexes to all BFc end groups and the dendrimer–β-CD assemblies are adsorbed at β-CD SAMs on gold. The dendrimers formed stable monolayers at the host surface owing to the formation of multivalent host–guest complexes, which were quantified by electrochemical methods for all dendrimers and by SPR titrations in the case of G1-PPI-$(BFc)_4$.

These findings are in full agreement with our recently reported study of the binding behavior of Fc-functionalized dendrimers towards the molecular printboard.[19,21] However, the electrochemically controlled binding of the BFc dendrimers to β-CD and β-CD SAMs is different and complex compared with the binding of Fc dendrimers. The oxidation of only one iron center in the BFc–β-CD complex results in the dissociation of the host–guest complexes and desorption of the dendrimers from the host surface. In the mixed-valence state $Fe_2^{(II,III)+}$ the BFc moiety is only able to form weak inclusion complexes with β-CD. This also caused a dramatic change in the redox processes of the dendrimers at the host surface. At bare gold electrodes the BFc moieties were all oxidized, first to $Fe_2^{(II,III)+}$ and subsequently to $Fe_2^{(III,III)2+}$. At the host surface three oxidation waves were observed. The first oxidation process only resulted in the oxidation of the bound BFc moieties while during the second oxidation step the remaining BFc moieties were oxidized leading to $Fe_2^{(II,III)+}$ for all BFc groups. Finally, during the third oxidation step all end groups undergo a second oxidation leading to molecules with all moieties in the $Fe_2^{(III,III)2+}$ state. Thus, the redox chemistry is strongly influenced by the ability of the BFc moiety to form inclusion complexes with β-CD.

Electronically communicating materials may lead to the development of new and interesting devices. The combination of self-assembly, multivalency, and redox activity allows the interactions of molecules to be altered and controlled. A detailed understanding of the redox processes of molecules on surfaces is a prerequisite for applications in, for instance, molecular electronics. Metal–SAM–metal junctions consisting of β-CD SAMs and monolayers of redox-active dendrimers are currently being investigated in our laboratories.

Experimental Section

General procedures: All moisture-sensitive reactions were carried out under argon. Reagents were commercially available and used without further purification. All dry solvents were prepared according to standard procedures and stored over molecular sieves. ^{1}H and ^{13}C NMR spectra were recorded on a Bruker AC300 or AMX400 spectrometer. Chemical shifts are reported in ppm downfield from TMS as internal standard. Matrix-assisted laser desorption ionization (MALDI) time-of-flight (TOF) mass spectra were recorded using a Perkin Elmer/PerSeptive Biosystems Voyager-DE-RP MALDI-TOF mass spectrometer. Analytical TLC was performed using Merck-prepared plates (silica gel 60 F-254 on aluminum). Merck silica gel (40–63 μm) was used for flash chromatography. Column chromatography was performed using silica gel (E. Merck, 0.040–0.063 mm, 230–240 mesh). Chloromercurioferrocene,[30] iodoferrocene,[30] and biferrocene[31] were prepared according to literature procedures.

Synthesis

4-Biferrocenyl-4-oxobutyric acid (5): A mixture of biferrocene (0.5 g, 1.4 mmol) and succinic anhydride (0.16 g, 1.5 mmol) was dissolved in CH_2Cl_2 and cooled to 0 °C. Aluminum trichloride (0.45 g, 3.4 mmol) was added to the solution as a powder and the reaction mixture was stirred overnight at room temperature. Subsequently, 10 % aqueous hydrochloric acid (50 mL) was added and stirring was continued for 1 h. The organic layer was separated and washed with 10 % hydrochloric acid (3 × 50 mL) after which the organic extract was dried with $MgSO_4$. Removal of solvent in vacuo gave a dark brown oil that was purified by column chromatography over silica, eluent 5 % MeOH/95 % CH_2Cl_2, and isolated as a dark red-brown oil (0.24 g, 32 %). M.p. 151.5–152 °C; ^{1}H NMR (400 MHz, $CDCl_3$): δ = 2.60 (t, J = 6.7 Hz, 2H; CH_2COOH), 2.81 (t, J = 6.3 Hz, 2H; CH_2CO), 3.9 (s, 5H; Cp), 4.22 (t, J = 1.7 Hz, 4H; Cp), 4.25 (t, J = 1.7 Hz, 4H; Cp), 4.36 (t, J = 1.7 Hz, 2H; Cp), 4.37 (t, J = 1.9 Hz, 2H; Cp), 4.41 (t, J = 1.7 Hz, 2H; Cp), 4.62 ppm (t, J = 1.9 Hz, 2H; Cp); ^{13}C NMR (100 MHz, $CDCl_3$): δ = 28.0 (CH_2COOH), 34.3 (CH_2CO), 66.6 (Cp), 67.6 (Cp), 68.5 (Cp), 69.5 (Cp), 70.4 (Cp), 71.4 (Cp), 73.3 (Cp), 79.2 (Cp), 81.5 (Cp), 86.9 (Cp), 170.0 (CO), 200.0 ppm (BFc*C*O); FAB MS: m/z calcd for $C_{24}H_{22}O_3Fe_2$: 470.14; found: 470.1 [M+H]; elemental analysis calcd (%) for $C_{24}H_{22}O_3Fe_2$: C 61.32, H 4.72; found: C 61.37, H 4.68.

Pentafluorophenyl 4-biferrocenyl-4-oxobutyrate (6): A mixture of the carboxylic acid **5** (0.6 g, 1.3 mmol), pentafluorophenol (0.29 g, 1.6 mol), and DCC (0.32 g, 1.6 mmol) was dissolved in dry THF (150 mL). The reaction was maintained under nitrogen for 48 h at room temperature. The THF was removed in vacuo and the remainder was dissolved in CH_2Cl_2 and washed thrice with saturated $NaHCO_3$ (ca. 50 mL). The organic extract was dried with $MgSO_4$ and concentrated and purified by column chromatography over silica gel with CH_2Cl_2 as eluent to give the final product as a red solid (0.5 g, 60 %). M.p. 125.5–126 °C; ^{1}H NMR (300 MHz, $CDCl_3$): δ = 2.86 (s, 4H; CH_2CH_2), 3.96 (2, 5H; Cp), 4.22 (t, J = 1.7 Hz, 2H; Cp), 4.24 (t, J = 1.8 Hz, 2H; Cp), 4.35 (t, J = 1.7 Hz, 2H; Cp), 4.36 (t, J = 1.9 Hz, 2H; Cp), 4.41 ppm (t, J = 1.8 Hz, 2H; Cp); ^{13}C NMR (100 MHz, $CDCl_3$): δ = 27.1 (O(CO)CH_2), 34.3 (CH_2CO), 66.7 (Cp), 67.6 (Cp), 68.5 (Cp), 69.6 (Cp), 70.4 (Cp), 71.4 (Cp), 73.4 (Cp), 79.2 (Cp), 81.5 (Cp), 86.9 (Cp), 136.4 (CF), 138.0 (CF), 141.3 (CF), 143.2 (CF), 169.6 (CO), 200.6 ppm (BFc*C*O); FAB MS: m/z calcd for $C_{30}H_{21}O_3F_5Fe_2$: 636.19; found: 637.4 [M+H]; elemental analysis calcd (%) for $C_{30}H_{21}O_3F_5Fe_2$ (636.1854): C 56.64, H 3.33, F 14.93: found: C 56.54, H 3.36, F 13.15.

G1-PPI-$(BFc)_4$ (7a): A mixture of **6** (300 mg, 0.47 mmol) and G1-PPI-$(NH_2)_4$ (32 mg, 0.10 mmol) dissolved in a small amount of dry chloroform was maintained under nitrogen and stirred overnight at room temperature. The product was isolated by repeated precipitation from hexane. Yield: 0.202 g, 95 %; ^{1}H NMR (300 MHz, $CDCl_3$): δ = 1.38 (br, 4H; $NCH_2CH_2CH_2CH_2N$), 1.70 (br, 8H; CH_2CH_2N), 2.37 (br, 8H; NHCOCH_2), 2.62 (br, 12H; CH_2NCH_2), 2.82 (br, 8H; CH_2CO), 3.24 (br, 8H; NHCH_2), 3.93 (s, 20H; Cp), 4.15 (br, 8H; Cp), 4.19 (br, 8H; Cp), 4.27 (br, 8H; Cp), 4.31 (br, 8H; Cp), 4.37 (br, 8H; Cp), 4.56 ppm (br, 8H; Cp); ^{13}C NMR (100 MHz, $CDCl_3$): δ = 23.5, 25.3, 30.1, 35.0, 37.5, 51.0, 53.3, 66.5, 67.6, 68.4, 69.5, 70.3, 71.4, 73.7, 79.3, 81.6, 86.8, 173.2 (NHCO), 203.5 ppm (BFcCO); MALDI-TOF MS: m/z calcd for $C_{112}H_{120}Fe_8N_6O_8$: 2125.02; found: 2126 [M+H].

G2-PPI-$(BFc)_8$ (7b): Following a procedure similar to that described for the synthesis of **G1-PPI-$(BFc)_4$** but by using G2-PPI-$(NH_2)_8$ (39 mg, 0.050 mmol) yielded **7b** (0.151 g, 69 %). ^{1}H NMR (300 MHz, $CDCl_3$): δ = 1.38 (br, 4H; $NCH_2CH_2CH_2CH_2N$), 1.70 (br, 28H; CH_2CH_2N), 2.37 (br, 16H; NHCOCH_2), 2.62 (br, 36H; CH_2NCH_2), 2.82 (br, 16H; CH_2CO), 3.24 (br, 16H; NHCH_2), 3.93 (s, 40H; Cp), 4.15 (br, 16H; Cp), 4.19 (br, 16H; Cp), 4.27 (br, 16H; Cp), 4.31 (br, 16H; Cp), 4.37 (br, 16H; Cp), 4.56 ppm (br, 16H; Cp); ^{13}C NMR (100 MHz, $CDCl_3$) δ = 22.2, 25.7, 30.0, 35.0, 37.5, 51.0, 66.6, 67.6, 68.4, 69.5, 70.3, 71.4, 73.8, 79.3, 81.6, 86.8, 173.4

(NHCO), 203.4 ppm (BFcCO); MALDI-TOF MS: m/z calcd for $C_{232}H_{256}Fe_{16}N_{14}O_{16}$: 4390.26; found: 4393 [$M$+H].

G3-PPI-(BFc)$_{16}$ (7c): Following a procedure similar to that described for the synthesis of **G1-PPI-(BFc)$_4$** but by using G2-PPI-$(NH_2)_8$ (44 mg, 0.026 mmol) yielded **7c** (0.200 g, 86 %). ^{1}H NMR (300 MHz, $CDCl_3$): δ = 1.37 (br, 4H; $NCH_2CH_2CH_2CH_2N$), 1.67 (br, 56H; CH_2CH_2N), 2.38 (br, 32H; $NHCOCH_2$), 2.54 (br, 36H; CH_2NCH_2), 2.82 (br, 32H; CH_2CO), 3.23 (br, 32H; $NHCH_2$), 3.92 (s, 80H; Cp), 4.14 (br, 32H; Cp), 4.18 (br, 32H; Cp), 4.26 (br, 32H; Cp), 4.30 (br, 32H; Cp), 4.37 (br, 32H; Cp), 4.56 ppm (br, 32H; Cp); ^{13}C NMR (100 MHz, $CDCl_3$): δ = 22.8, 26.0, 30.1, 35.1, 37.8, 51.2, 66.6, 67.7, 68.4, 69.5, 70.3, 71.4, 73.8, 79.3, 81.7, 86.7, 173.0 (NHCO), 203.3 ppm (BFcCO); MALDI-TOF MS: m/z calcd for $C_{472}H_{528}Fe_{32}N_{30}O_{32}$: 8920.76; found: 8945 [$M$+Na].

Materials and methods: All glassware used to prepare the monolayers was immersed in a piranha solution (conc. H_2SO_4/33 % H_2O_2, 3:1). *Warning*: piranha should be handled with caution: it can detonate unexpectedly.[44] Next, the glassware was rinsed with large amounts of Milli-Q water. All adsorbate solutions were prepared immediately prior to use. All solvents used in monolayer preparations were of p.a. grade.

Substrate preparation: Glass-supported gold substrates for SPR spectroscopy and electrochemistry (2.54 cm diameter, 47.5 and 200 nm metal thickness, respectively, with a 2 nm titanium adhesion layer) were obtained from SSENS BV (Hengelo, The Netherlands). Gold substrates were cleaned by brief immersion in the piranha solution and the resulting oxide layer was removed by leaving the substrates for 10 min in absolute EtOH. The substrates were subsequently immersed in the adsorbate solution (0.1–1 mM) for around 16 h at 60 °C. Next, the samples were removed from the solutions and rinsed thoroughly with chloroform, ethanol, and Milli-Q water. Adsorption of the dendrimers was carried out by immersing a β-CD SAM on gold in an aqueous solution of the corresponding dendrimer–β-CD assembly (0.1 mM in BFc functionality in the presence of 10 mM β-CD at pH 2) for at least 1 h. Subsequently the samples were thoroughly rinsed with Milli-Q water (at pH 2 to ensure full protonation of the amines) and dried in a stream of nitrogen.

Isothermal titration calorimetry: Titrations were performed at 25 °C using a Microcal VP-ITC titration microcalorimeter. Sample solutions were prepared using Milli-Q water. Titrations were performed by adding aqueous β-CD solutions (10 or 5 mM) at pH 12 to 4-biferrocenyl-4-oxobutyric acid (1 or 0.5 mM) at the same pH. The titrations were analyzed using a least-squares fitting procedure.

Electrochemistry: Electrochemical measurements were performed with an AUTOLAB PGSTAT10 instrument in a custom-built three-electrode setup equipped with a platinum counter electrode, a mercury sulfate reference electrode ($V_{MSE} = +0.61 V_{NHE}$), and with a screw cap holding the gold working electrode (area exposed to the solution = 0.44 cm^2). Cyclic voltammograms of immobilized dendrimers at the β-CD SAMs were recorded in an aqueous 0.1 M K_2SO_4 solution between $-0.35 V_{MSE}$ and $0.5 V_{MSE}$ or $0.6 V_{MSE}$ at scan rates of 0.05, 0.010, 0.025, 0.05, 0.1, 0.2, 0.5, 1, 2, 5, and 10 V s^{-1}. Cyclic voltammograms of the dendrimer–β-CD assemblies in solution (10 mM β-CD at pH 2) at concentrations of 0.5, 0.2, and 0.2 mM in BFc functionality for **7a**, **7b**, and **7c**, respectively, at bare gold electrodes and at β-CD SAMs at gold were recorded at scan rates varying from 1 mV s^{-1} to 0.5 V s^{-1}. For DPV a modulation time of 0.5 s, interval time of 0.2 s, a step potential of 1 mV, and a modulation amplitude of 10 mV were used.

Combined electrochemistry and SPR spectroscopy: The electrochemistry/SPR setup was very similar to that described previously by Knoll and co-workers.[43] The SPR setup in the Kretschmann[45] configuration was obtained from Resonant Probes GmbH. The beam of a NeHe laser (JDS Uniphase, 10 mW, λ = 633 nm) passes through a chopper that is connected to a lock-in amplifier (EG&G, 7256). The modulated beam then passes through two polarizers (Owis), which can be used to adjust the intensity and the plane of polarization of the laser. Then the beam is reflected off the base of the coupling prism (Scott, LASFN9) and focused by a lens (50 mm, Owis) into a photodiode detector.

The glass-supported gold SPR substrates at the prism were clamped against a Teflon cuvette with O-rings providing liquid-tight seals. The CV measurement was performed with an AUTOLAB PGSTAT10 instrument in a three-electrode setup with the gold SPR substrates at the prism as the working electrode, a Ag/AgCl reference electrode, and a platinum wire as counter electrode. The CV-induced desorption processes on gold were detected by monitoring reflectivity changes as a function of time at a fixed incident angle θ.

Acknowledgements

The Dutch Technology Foundation STW is gratefully acknowledged for funding the Simon Stevin Award project on Nanolithography (grant no. TST 4946 to D.N.R.). Karolina Dolatowska (Warsaw University of Technology) received a Socrates grant to study at the University of Twente. We are grateful to Dr. Bernard Boukamp and Dr. Aldrik Velders for useful discussions.

[1] a) C. Joachim, J. K. Gimzewski, A. Aviram, *Nature* **2000**, *408*, 541; b) J. M. Tour, *Acc. Chem. Res.* **2000**, *33*, 791.
[2] a) A. D. Mehta, M. Rief, J. A. Spudich, *Science* **1999**, *283*, 1689; b) S. Weiss, *Science* **1999**, *283*, 1676.
[3] a) M. Granström, K. Petritsch, A. C. Arias, A. Lux, M. R. Andersson, R. H. Friend, *Nature* **1998**, *395*, 257; b) C. J. Brabec, N. S. Sariciftci, J. C. Hummelen, *Adv. Funct. Mater.* **2001**, *11*, 15.
[4] a) H. Nakamura, I. Karube, *Anal. Bioanal. Chem.* **2003**, *377*, 446; b) H. C. Pirrung, *Angew. Chem.* **2002**, *114*, 1326; *Angew. Chem. Int. Ed.* **2002**, *41*, 1286; c) B. S. Wilson, S. Nock, *Angew. Chem.* **2003**, *115*, 510; *Angew. Chem. Int. Ed.* **2003**, *42*, 494.
[5] J. Huskens, M. A. Deij, D. N. Reinhoudt, *Angew. Chem.* **2002**, *114*, 4647; *Angew. Chem. Int. Ed.* **2002**, *41*, 4467.
[6] T. Auletta, B. Dordi, A. Mulder, A. Sartori, S. Onclin, C. M. Bruinink, M. Péter, C. A. Nijhuis, H. Beijleveld, H. Schönherr, G. J. Vancso, A. Casnati, R. Ungaro, B. J. Ravoo, J. Huskens, D. N. Reinhoudt, *Angew. Chem.* **2004**, *116*, 373; *Angew. Chem. Int. Ed.* **2004**, *43*, 369.
[7] C. M. Bruinink, C. A. Nijhuis, M. Péter, B. Dordi, O. Crespo-Biel, T. Auletta, A. Mulder, H. Schönherr, G. J. Vancso, J. Huskens, D. N. Reinhoudt, *Chem. Eur. J.* **2005**, *11*, 3988.
[8] a) M. J. W. Beulen, J. Bügler, B. Lammerink, F. A. J. Geurts, E. M. E. F. Biemond, K. G. C. Leerdam, F. C. J. M. Van Veggel, J. F. J. Engbersen, D. N. Reinhoudt, *Langmuir* **1998**, *14*, 6424; b) M. J. W. Beulen, J. Bügler, M. R. De Jong, B. Lammerink, J. Huskens, H. Schönherr, G. J. Vancso, B. A. Boukamp, H. Wieder, A. Offenhäuser, W. Knoll, F. C. J. M. van Veggel, D. N. Reinhoudt, *Chem. Eur. J.* **2000**, *6*, 1176.
[9] S. Onclin, A. Mulder, J. Huskens, B. J. Ravoo, D. N. Reinhoudt, *Langmuir* **2004**, *20*, 5460.
[10] J. Huskens, A. Mulder, T. Auletta, C. A. Nijhuis, M. J. W. Ludden, D. N. Reinhoudt, *J. Am. Chem. Soc.* **2004**, *126*, 6784.
[11] M. Mammen, S.-K. Choi, G. M. Whitesides, *Angew. Chem.* **1998**, *110*, 2908; *Angew. Chem. Int. Ed.* **1998**, *37*, 2754.
[12] a) J. F. G. A. Jansen, E. M. M. De Brabander-Van den Berg, E. W. Meijer, *Science* **1994**, *266*, 1226; b) M. W. P. L. Baars, P. E. Froehling, E. W. Meijer, *Chem. Commun.* **1997**, 1959; c) G. Pistolis, A. Malliaris, D. Tsiourvas, C. M. Paleos, *Chem. Eur. J.* **1999**, *5*, 1440.
[13] O. Crespo-Biel, B. Dordi, D. N. Reinhoudt, J. Huskens, *J. Am. Chem. Soc.* **2005**, *127*, 594.
[14] a) J. J. Michels, J. Huskens, D. N. Reinhoudt, *J. Chem. Soc., Perkin Trans. 2* **2002**, 102; b) R. M. Crooks, B. I. Lemon III, L. Sun, L. Lee, K. Yeung, M. Zhao, *Top. Curr. Chem.* **2001**, *212*, 81.
[15] a) M.-C. Daniel, J. Ruiz, S. Nlate, J.-C. Blais, D. Astruc, *J. Am. Chem. Soc.* **2003**, *125*, 2617; b) W. Ong, M. Gomez-Kaifer, A. E. Kaifer, *Chem. Commun.* **2004**, 1677.
[16] E. R. Gillies, J. M. J. Fréchet, *J. Am. Chem. Soc.* **2002**, *124*, 14137.
[17] M. Ooe, M. Murata, T. Mizugaki, K. Ebitani, K. Kaneda, *Nano Lett.* **2002**, *2*, 999.
[18] A. M. Bittner, X. C. Wu, K. Klaus, *Adv. Funct. Mater.* **2002**, *12*, 432.

[19] C. A. Nijhuis, J. Huskens, D. N. Reinhoudt, *J. Am. Chem. Soc.* **2004**, *126*, 12266.
[20] A. E. Kaifer, *Acc. Chem. Res.* **1999**, *32*, 62.
[21] C. A. Nijhuis, F. Yu, W. Knoll, J. Huskens, D. N. Reinhoudt, *Langmuir* **2005**, *21*, 7866.
[22] a) A. S. Abd-El-Aziz, I. Manners, *J. Inorg. Organomet. Polym.* **2005**, *15*, 157; b) P. Nguyen, P. Gómez-Elipe, I. Manners, *Chem. Rev.* **1999**, *99*, 1515; c) S. Zou, M. A. Hempenius, H. Schönherr, G. J. Vancso, *Macromol. Rapid Commun.* **2006**, *27*, 103.
[23] a) S. Barlow, D. O'Hare, *Chem. Rev.* **1997**, *97*, 637; b) H. Nishihara, M. Murata, *J. Inorg. Organomet. Polym.* **2005**, *15*, 147.
[24] I. Cuadrado, C. M. Casado, B. Alonso, M. Morán, J. Losanda, V. Belsky, *J. Am. Chem. Soc.* **1997**, *119*, 7613.
[25] J. Alvarez, T. Ren, A. E. Kaifer, *Organometallics* **2001**, *20*, 3543.
[26] H. Nishihara, *Bull. Chem. Soc. Jpn.* **2001**, *74*, 19.
[27] T.-Y. Dong, C.-K. Chang, C.-H. Cheng, S.-H. Lee, L.-L. Lai, M. Y.-N. Chiang, K.-J. Lin, *Organometallics* **1997**, *16*, 5816.
[28] a) M. Yamada, H. Nishihara, *Langmuir* **2003**, *19*, 8050; b) T.-Y. Dong, L.-S. Chang, I.-M. Tseng, S.-J. Huang, *Langmuir* **2004**, *20*, 4471; c) H.-W. Shih, T.-Y. Dong, *Inorg. Chem. Commun.* **2004**, *7*, 646.
[29] T.-Y. Dong, C.-K. Chang, C.-H. Cheng, K.-J. Lin, *Organometallics* **1999**, *18*, 1911.
[30] R. W. Fish, M. Rosenblum, *J. Org. Chem.* **1965**, *30*, 1253.
[31] M. D. Rausch, *J. Org. Chem.* **1961**, *26*, 1802.
[32] M. V. Rekharsky, Y. Inoue, *Chem. Rev.* **1998**, *98*, 1875.
[33] M. R. De Jong, J. Huskens, D. N. Reinhoudt, *Chem. Eur. J.* **2001**, *7*, 4164,
[34] J. J. Michels, M. W. P. L. Baars, E. W. Meijer, J. Huskens, D. N. Reinhoudt, *J. Chem. Soc., Perkin Trans. 2* **2000**, 1914.
[35] P. Zanello, *Inorganic Electrochemistry: Theory, Practice and Application*, The Royal Society of Chemistry, Cambridge, **2003**.
[36] a) G. R. Newkome, E. He, C. N. Moorefield, *Chem. Rev.* **1999**, *99*, 1689; b) I. Cuardo, M. Morán, C. M. Casado, B. Alonso, J. Losada, *Coord. Chem. Rev.* **1999**, *193–105*, 395.
[37] a) S. Nlate, J. Ruiz, J.-C. Blais, D. Astruc, *Chem. Commun.* **2000**, 417; b) S. J. Green, J. J. Pietron, J. J. Stokes, M. J. Hostetler, H. Vu, W. P. Wuelfing, R. W. Murray, *Langmuir* **1998**, *14*, 5612.
[38] W. Knoll, *Annu. Rev. Phys. Chem.* **1998**, *49*, 569.
[39] A. Mulder, T. Auletta, A. Sartori, S. Del Ciotto, A. Casnati, R. Ungaro, J. Huskens, D. N. Reinhoudt, *J. Am. Chem. Soc.* **2004**, *126*, 6627.
[40] M. R. De Jong, J. Huskens, D. N. Reinhoudt, *Chem. Eur. J.* **2001**, *7*, 4164.
[41] T. Matsue, D. H. Evans, T. Osa, N. Kobayashi, *J. Am. Chem. Soc.* **1985**, *107*, 3411.
[42] A. J. Bard, L. R. Faulkner, *Electrochemical Methods: Fundamentals and Applications*, Wiley, New York, **2001**.
[43] a) C. Xia, R. C. Advincula, A. Baba, W. Knoll, *Langmuir* **2002**, *18*, 3555; b) A. Baba, M.-K. Park, R. C. Advincula, W. Knoll, *Langmuir* **2002**, *18*, 4648; c) A. Baba, R. C. Advincula, W. Knoll, *J. Phys. Chem. B* **2002**, *106*, 1581; d) E. F. Aust, S. Ito, M. Sawondny, W. Knoll, *Trends Polym. Sci.* **1994**, *2*, 313.
[44] D. A. Dobbs, R. G. Bergman, K. H. Theopold, *Chem. Eng. News* **1990**, *68*, 2.
[45] A. T. M. Lenferink, R. P. H. Kooyman, J. Greve, *Sens. Actuators B* **1991**, *3*, 261.

Received: June 3, 2006
Published online: October 16, 2006

